

# **SPATIAL STATISTICS OF PARTICLE CLUSTERS AND MODELING OF PITTING CORROSION**

D.G. Harlow and R.P. Wei

Mechanical Engineering and Mechanics, Lehigh University,  
19 Memorial Drive West, Bethlehem, PA 18015-3085, USA

## **ABSTRACT**

Localized (pitting) corrosion is recognized as a primary degradation mechanism that affects the durability and integrity of structures made of aluminum alloys, and it is a concern for commercial transport and military aircraft. Corrosion pits have been shown to commence at constituent particles, and to evolve into severe pits by growth through clusters of these particles in the alloys. These severe pits serve as nucleation sites for subsequent corrosion fatigue cracking. Thus, the role of clusters of constituent particles is critical to the quality of aluminum alloys subjected to deleterious environments. To formulate a stochastic model of corrosion, as a part of the methodology for structural reliability analysis, it is essential to have quantitative descriptions of the spatial statistics of the particles and particle clusters, including their location, size, density and chemical composition. A simple probability model incorporating the role of clustered particles on the growth of corrosion pits is presented and discussed. The proposed model includes the effect of randomness in the number and sizes of the clusters. The applicability of the model is considered in terms of experimental data from 2024-T3 aluminum alloy specimens that had been exposed to a 0.5 M NaCl solution.

## **KEYWORDS**

Particle statistics, Cluster statistics, Aluminum alloys, Corrosion, Pitting corrosion, Probability modeling

## **INTRODUCTION**

Pitting corrosion in aluminum alloys has been recognized as a significant degradation mechanism, specifically as a precursor to corrosion fatigue crack initiation and growth, that impacts the reliability, durability, and integrity of both military and commercial aircraft [1-4]. It has been shown that pitting results from the galvanic coupling of constituent particles with the alloy matrix [5-9]. Pit growth is a stochastic process that depends upon material properties and environmental conditions. In fact, severe pits with depths greater than 20  $\mu\text{m}$  have been observed as nuclei for the early onset of fatigue crack growth and subsequent reductions in fatigue life.

The scanning electron microscopy (SEM) micrograph in Fig. 1(a) shows a typical pit that resulted from the galvanic coupling between a surface particle and the matrix. The complex geometrical structure of a severe corrosion pit is illustrated by the SEM micrographs in Fig. 1(b) and (c) of an epoxy replica of a typical severe pit. The rounded features on the surface correspond to individual constituent particles, and indicate that the

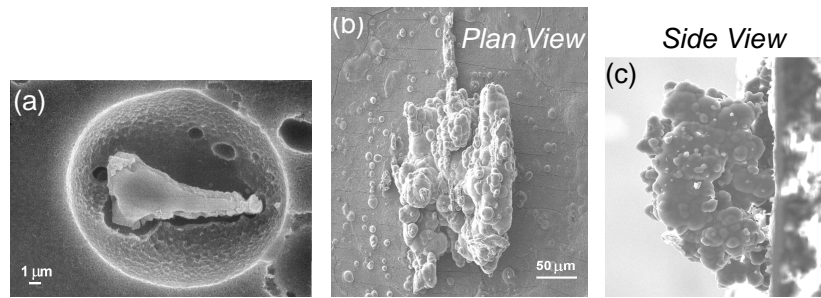


**Figure 1:** SEM micrographs – (a) particle induced corrosion pit; and epoxy replica of a severe corrosion pit: (b) plan (bottom) and (c) side (elevation) views relative to the original pit in a 2024-T3 aluminum alloy sheet [1,6,8].

pit evolved by progressive particle-induced dissolution through a cluster of particles. Thus, the size and location of particle clusters is an essential component in the stochastic evolution of pitting. The purpose here is to incorporate spatial statistics of constituent particles and clusters of particles into a simple mechanistically based probability model for corrosion pit growth.

Polished sections of 2024-T3 aluminum alloy, the area of which was approximately  $340 \mu\text{m} \times 1030 \mu\text{m}$ , were observed using SEM. In order to estimate accurately the particle geometry and clustering for the alloy, observations were made on the LS, TS, and LT surfaces. One area was considered on each of the LS and TS surfaces, but two different areas were observed of the LT surface. Subsequently, the same two areas about  $20 \mu\text{m}$  deeper were analyzed on the LT surface. The average numbers of particles per  $\text{mm}^2$ , with an area of at least  $0.5 \mu\text{m}^2$ , were found to be 3850, 3820, and 3180 for the LS, TS, and LT surfaces, respectively. Detailed properties for this alloy may be found in [1].

## PARTICLE STATISTICS

Figure 2 is an SEM micrograph of an LT surface that is typical of polished specimens of 2024-T3 aluminum alloy, and it illustrates the inherent randomness in the number, size, and location of the constituent particles. It is impossible to describe adequately this complex spatial pattern from observations alone. Certainly, there is no apparent spatial structure, and the need for modeling is manifest. Many different models have been suggested for irregularly shaped and randomly distributed particles [10]. The primary concern herein is the statistical description of particle clustering that reflects not only geometrical, but also electrochemical considerations induced by deleterious environments. It has been shown, using spatial statistics, that the constituent particles in 2024-T3 are statistically clustered [11], and that was confirmed for the material used herein. Furthermore, it has been demonstrated that corrosion pits are statistically, regularly spaced because pitting encompasses several clustered particles [11].

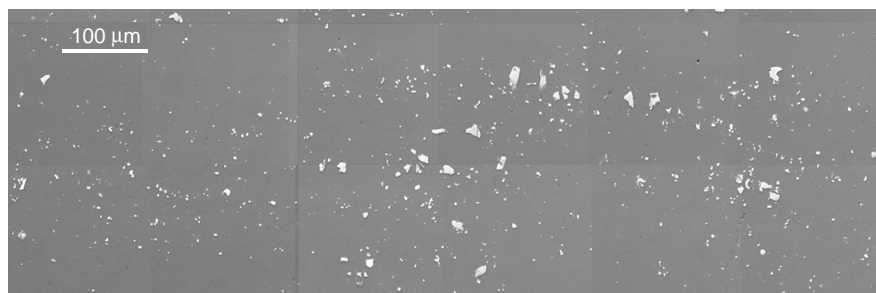


**Figure 2:** Typical SEM micrograph of a polished section of the LT surface of 2024-T3 aluminum alloy.

One of the key random variables (rvs) for the ensuing probability computations is the particle area  $A_p$ . The cumulative distribution function (cdf) for  $A_p$  was estimated from the observation of over 7,000 particles. The truncated two-parameter Frechet cdf, given by

$$F(x) = \exp\{-(x/\beta)^{-\alpha} - (\delta/\beta)^{-\alpha}\}, \quad x \geq 0, \quad \alpha > 0, \quad \beta > 0, \quad \delta > 0, \quad (1)$$

where  $\alpha$  is the shape parameter,  $\beta$  is the scale parameter and  $\delta$  is the maximum value, was fit using maximum likelihood estimation (MLE) [12]. This Frechet cdf was selected because it characterizes the maxima of rvs. Since the largest particles induce the most severe damage, it is preferred. Furthermore, the geometrical features of the material necessarily have an upper bound. The Frechet MLE estimates are acceptable for the data with a confidence level of 99%, based on the Kolmogorov-Smirnov (K-S) goodness-of-fit test [12]. Using the likelihood ratio test [12] with a confidence over 97.5%, the six data sets may be merged, which is evidence that  $A_p$  for each surface is statistically similar. The estimates for the merged data for  $A_p$  are as follows:  $\hat{\alpha} = 2.0$ ,  $\hat{\beta} = 5.1 \mu\text{m}^2$ ,  $\hat{\delta} = 285.7 \mu\text{m}^2$ ,  $\hat{\mu} = 5.8 \mu\text{m}^2$ , and  $c\hat{\nu} = 52\%$ , where  $\mu$  is the mean and  $c\nu$  is the coefficient of variation. Note that the scatter is large, which indicates extensive variability in particle sizes.

## MODELING THE CLUSTER SIZE FOR CONSTITUENT PARTICLES

It has been demonstrated that the galvanic current induced from a particle subjected to a deleterious environment has a “throwing power” radius that can be approximated by  $ma_p$ , where  $m$  is an appropriate multiple ranging from 2 to 4 [13] and  $a_p$  is the particle radius. If additional particles are within that distance, galvanic dissolution will continue, thus propagating pitting corrosion. Herein, two particles are considered to be in the same cluster if the distance between their centroids is less than  $ma_p$ . Consequently, the cluster size is estimated by counting the total number of particles  $n_{pc}$  that satisfy this pair-wise criterion. In order for a severe corrosion pit to form,  $n_{pc}$  must be sufficiently large to sustain the galvanic dissolution needed for pit growth. It is assumed that  $n_{pc} \geq 4$  is reasonable, and empirically such an assumption matches statistical observation quite well. Figure 3 shows the centroid for each particle in Fig. 2. The polygons shown on the figure are schematic approximations for the effective area of each cluster according to this criterion for which  $m = 3$  and  $n_{pc} \geq 4$ . The cluster areas exhibit considerable scatter. Since each point is sized equally, the figure is somewhat deceiving. Also, the polygons are rough approximations for the cluster area. Refer to Fig. 1 for a typical cluster. Again, the cdf of Eqn. 1 is a very good characterization for the particle cluster radius  $a_{pco}$ , which is another critical rv for the probability analysis. All six sets of cluster radii are very tight, and they may be merged according to the likelihood ratio test for any confidence greater than 70%. Thus,  $a_{pco}$  for the LT, LS, and TS planes may be considered to be statistically identical with parameters of  $\hat{\alpha} = 1.8$ ,  $\hat{\beta} = 14.3 \mu\text{m}$ ,  $\hat{\delta} = 42.2 \mu\text{m}$ ,  $\hat{\mu} = 14.4 \mu\text{m}$ , and  $c\hat{\nu} = 50\%$ . Based on the K-S goodness-of-fit test, any confidence greater than 70% is appropriate for the fit. The large  $c\hat{\nu}$  for the clusters is confirmed graphically on Fig. 3.

Given the clustering criterion, the number of particles per cluster  $n_{pc}$  is well characterized by the discrete

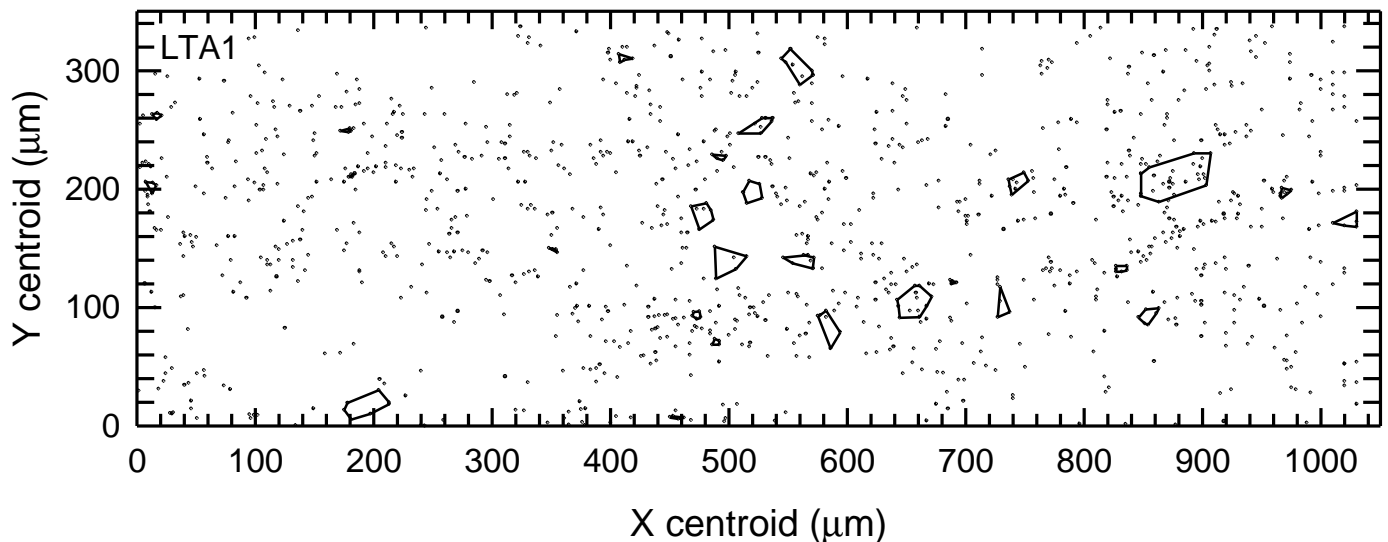


**Figure 3:** Schematic representation of the particle centroids and clusters for the LT surface in Figure 2.

Pareto distribution [14] given by

$$p_k = \Pr\{n_{pc} = k\} = ck^{-(\rho+1)}; \quad k \geq 1, \quad (2)$$

with any confidence greater than 70% using the K-S test. The estimated parameters are  $\hat{c} = 2.8$  and  $\hat{\rho} = 1.7$ . Since the cluster area is small, it is assumed that in its related volume the particle distribution is uniformly distributed. Thus, the local volume particle density is assumed to be equal to the area particle density.

## SIMPLIFIED MODELING OF CORROSION PITTING

Plausible models for particle induced pitting have been explored [14]. A simplified model for pit growth was adopted and used, with success, in exploring the implications of pitting corrosion on the evolution of corrosion and fatigue damage in high-strength aluminum alloys and in aircraft that had been in long-term commercial service [4,15]. Although there is ample experimental support for this model for characterizing pitting corrosion around an isolated particle, or a small cluster of particles at the surface, its extension to describe the development and growth of a severe corrosion pit is problematic. The pitting current cannot be constant, as assumed above; it must reflect the galvanic dissolution of the alloy matrix through its coupling with the entire cluster of constituent particles that are progressively exposed by pitting [13]. The model envisions pit growth to be sustained by galvanic current from a small group of constituent particles that are exposed at the surface to initiate pit growth.

For simplicity, the model assumed the pit to be hemispherical in shape, with radius  $a$ , and its growth would be at a constant volumetric rate, obeying Faraday's law. Specifically, the pit volume is  $V = (2/3)\pi a^3$ . The rate of pit growth is given in terms of Faraday's law, and the time evolution of pit size and the time required to reach a given pit size are determined from direct integration of the rate equation, and are as follows:

$$\frac{da}{dt} = \frac{da}{dV} \frac{dV}{dt} = \frac{1}{2\pi a^2} \frac{dV}{dt} = \frac{MI_{pit}}{2\pi n\rho F} \frac{1}{a^2}, \quad (3)$$

where  $M$  is the molecular weight;  $I_{pit}$  is the pitting current;  $n$  is the valence;  $\rho$  is the density;  $F$  is Faraday's constant ( $9.65 \times 10^7$  C/kg-mol). For aluminum,  $M = 27$  kg/kg-mol;  $n = 3$ ; and  $\rho = 2.7 \times 10^3$  kg/m<sup>3</sup>. For particle induced pitting,  $I_{pit}$  is defined by the cathodic current density that can be supported by the cluster of particles and their effective surface area.

Explicitly,  $I_{pit}$  is assumed to be given by the following:

$$I_{pit} = \sum_{i=1}^{n_{pc}} (i_{co})_i (2\pi a_p^2)_i, \quad (4)$$

where  $(i_{co})_i$  is the limiting cathodic current density for particle  $i$ ,  $(2\pi a_p^2)_i = (2A_p)_i$  is the surface area of particle  $i$  that is exposed to the electrolyte within a growing pit at time  $t$ , and  $n_{pc}$  is a rv for the number of particles that are exposed on the surface of a hemispherical pit of radius  $a$  at time  $t$ . The exposed portion of a cluster includes all of the constituent particles at the pit surface. Pit growth is sustained by the galvanic coupling current between the matrix constituting the pit surface and the exposed particles. Even though the particle composition and electrochemical conditions evolve for each particle in a pit,  $(i_{co})_i$  for  $i \geq 1$  are assumed herein to be identically distributed and are taken to be constant for simplicity.

Integrating Eqn. 3 leads to the following for the time evolution of cluster induced corrosion pitting:

$$a = \left[ \frac{3MI_{pit}}{2\pi n\rho F} t + a_{pco}^3 \right]^{1/3} \quad \text{and} \quad t = \frac{2\pi n\rho F}{3MI_{pit}} (a^3 - a_{pco}^3), \quad (5)$$

where  $a_{pco}$  is a rv for the initial pit size, *i.e.*, the size of the initiating cluster of particles.

## COMPUTATIONS, COMPARISONS, AND DISCUSSION

The rvs that play a key role in the following mechanistically based probability computations are  $(i_{co})_i$ ,  $a_{pco}$ ,  $n_{pc}$ , and  $(A_p)_i$ . The limiting values of  $(i_{co})_i$  depend on the composition of the particles and the electrochemical conditions within the pit, and it can range between 40 and 600  $\mu\text{A}/\text{cm}^2$ . To estimate the influences of particle composition, solution acidification, dealloying and copper deposition,  $\hat{\mu} = 200 \mu\text{A}/\text{cm}^2$  and  $c\hat{v} = 52\%$  were assumed for  $(i_{co})_i$  throughout; see [7,8]. The statistical properties of the other rvs were given above. In order to validate the model, computations were made and compared to experimentally measured pit depths that were formed in 2024-T3 aluminum alloy sheet specimens after immersion in 0.5M NaCl solution for 16 to 384 h [13]. The measured pit depths are shown as a function of exposure time on Fig. 4. The lines are probability percentile lines computed from the model given in Eqn. 5. The solid line is the median (50<sup>th</sup> percentile), whereas the lines with symbols are the percentiles appropriate for the 80%, 90%, and 95% confidence bands. The dashed line is the linear least squares regression through the data. The regression and median predicted from the mechanistically based probability model are very close over the range of the data, which is reassuring that the model has merit. The predicted lower confidence bounds agree well with the data. The deviation between the lower bounds is small because the data for the rvs in Eqn. 5 are skewed toward the lower tails of the cdfs. The 80% and 90% predicted upper bounds are also quite good; however, the 95% upper bound is quite broad. The divergence in these upper bounds is attributable to the large scatter in upper tails of the data for the rvs in Eqn. 5. In other words, in the upper percentiles of the data are very disperse and are considerably larger in magnitude than the preponderance of the data. Furthermore, longer exposures to deleterious environments may yield more variability than indicated by this data. Thus, additional investigations, both modeling and experimental, are warranted.

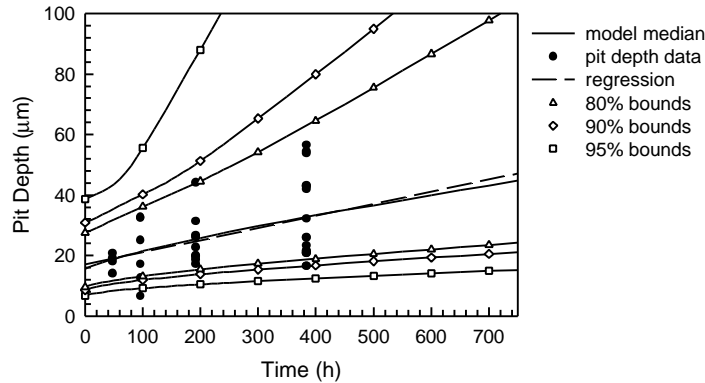


**Figure 4:** Pit depth data with the linear regression and 95% statistical confidence bounds and the median and 95% confidence bounds computed from the simplified pitting corrosion model.

The cdf for  $a$  given  $t$  also can be computed from Eqn. 3, and Fig. 5 shows selected cdfs plotted on Frechet probability paper as  $t$  varies. For  $t = 0$ , the graph is the cdf for  $a_{pco}$ , which is truncated at the maximum 42.2  $\mu\text{m}$ . The large variability in each cdf is evident, increasing with increasing  $t$ , which corroborates the broad confidence bounds in Fig. 4. Also as  $t$  increases, the cdfs become nearly linear, indicating that a two-parameter Frechet cdf, *i.e.*  $\delta = 0$ , would be an excellent approximation for these cdfs.

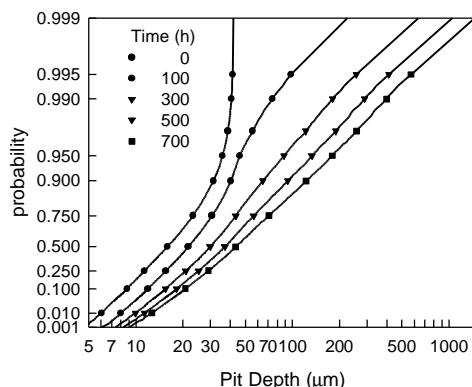


**Figure 5:** Evolution of the cdf for pit depth  $a$ .

## CONCLUSIONS

A simplified probabilistic model incorporating the role of clustered particles on the growth of corrosion pits has been presented and discussed. The proposed pit growth model includes the galvanic dissolution of the alloy matrix through its coupling with clusters of constituent particles that are progressively exposed by the pitting process. The merit of the model was considered by comparing model predictions to experimental data from 2024-T3 aluminum alloy specimens that had been exposed to a 0.5 M NaCl solution. The model predictions included estimations for the random variables that were obtained from independent measurements. The predicted median evolution and 90% confidence bounds agree well with the data. The effect of randomness in the number and sizes of the constituent particles and clusters of particles on pitting is quite pronounced. Thus, the role of clusters of constituent particles is critical to the quality of aluminum alloys subjected to deleterious environments. This effort provides a basis for a mechanistically based probability model for reliability analysis in life-cycle design and management of engineered systems when corrosion is the operative damage mechanism. Even so, additional pitting corrosion experiments and better modeling to account for material anisotropy and volume effects are planned for the future.

## ACKNOWLEDGMENTS

This research was supported by the Air Force Office of Scientific Research under Grant F49610-1-98-0198, and by the ALCOA Technical Center.

## REFERENCES

1. Chen, G.S., Gao M., and Wei R.P. (1996) *Corrosion* **52**, 8.
2. Chen, G.S., Wan, K.-C., Gao, M., Wei, R.P., and Flournoy, T.H. (1996) *Mats Sci. and Engr.* **A219** 126.
3. Harlow, D.G. and Wei, R.P. (1999) *Fatigue Fract. Engng Mater. Struct.* **22** 427.
4. Harlow, D.G. and Wei, R.P. (2001) *Fatigue Fract. Engng Mater. Struct.* (to appear).
5. Wei, R.P., Liao, C.-M., and Gao, M. (1998) *Metall. Mater. Trans.* **29A** 1153.
6. Liao, C.-M., Olive, J.M., Gao, M., and Wei, R.P. (1998) *Corrosion* **54** 451.
7. Gao, M., Feng, C.R., and Wei, R.P. (1998) *Metall. Mater. Trans.* **29A** 1145.
8. Liao, C.-M., Chen, G.S., and Wei, R.P. (1996) *Scripta Mater.* **35** 1341.
9. Liao, C.-M. and Wei, R.P. (1999) *Electrochimica Acta* **45** 881.
10. Cressie, N.A.C. (1991) *Statistics for Spatial Data*. Wiley, New York.
11. Cawley, N. and Harlow, D.G. (1996) *J. Mat. Sci.* **31** 5127.
12. Lawless, J. (1982) *Statistical Models and Methods for Lifetime Data*. Wiley, New York.
13. Wei, R.P. (2001) *Scripta Mater.* (to appear).
14. Harlow, D.G. and Wei, R.P. (1998) *Engr. Frac. Mech.* **59** 305.
15. Harlow, D.G. and Wei, R.P. (1994) *J. A.I.A.A.* **32** 2073.